






The conterminous United States are projected to become more prone to flash floods in a high-end emissions scenario

Zhi Li ¹, Shang Gao ¹, Mengye Chen¹, Jonathan J. Gourley ², Changhai Liu³, Andreas F. Prein ³ & Yang Hong ¹✉

Flash floods are largely driven by high rainfall rates in convective storms that are projected to increase in frequency and intensity in a warmer climate in the future. However, quantifying the changes in future flood flashiness is challenging due to the lack of high-resolution climate simulations. Here we use outputs from a continental convective-permitting numerical weather model at 4-km and hourly resolution and force a numerical hydrologic model at a continental scale to depict such change. As results indicate, US floods are becoming 7.9% flashier by the end of the century assuming a high-emissions scenario. The Southwest (+10.5%) has the greatest increase in flashiness among historical flash flood hot spots, and the central US (+8.6%) is emerging as a new flash flood hot spot. Additionally, future flash flood-prone frontiers are advancing northwards. This study calls on implementing climate-resilient mitigation measures for emerging flash flood hot spots.

¹School of Civil Engineering and Environmental Science, University of Oklahoma, Norman, OK 73072, USA. ²NOAA National Severe Storms Laboratory, Norman, OK 73072, USA. ³National Center for Atmospheric Research, Boulder, CO 80301, USA. ✉email: yanghong@ou.edu

Floods in the United States are the most devastating water-related natural hazards^{1–7}. According to the National Weather Service storm reports, floods have cost more than 159 billion US dollars and 2000 fatalities from 1996 to 2020 (last access: 27 July 2021), let alone immeasurable damage to ecosystems. Among all types of floods, flash floods are one of the most devastating subsets, accounting for nearly half of those economic losses^{6–8}. The central question for the hydrologic science community, practitioners, and more urgently the weather service agencies becomes: How do future floods evolve under a changing climate⁹?

Flood risks are largely tied to increased precipitation extremes induced by a warmer climate in addition to more direct anthropogenic effects^{10,11}. Although the Clausius-Clapeyron equation infers a theoretical 7% increase in atmospheric water holding capacity per degree Celsius warming¹², extreme precipitation might be increasing even more due to changes in storm structure¹³, storm dynamics¹⁴, and large-scale weather patterns¹⁵. Global Climate Models (GCMs), which are mainly designed for simulating large-scale climate variables, poorly represent mesoscale weather systems because of their coarse resolutions (>10 km) and insufficient parameterization schemes^{16,17}. GCM-based climate change-related flood studies are limited in assessing changes in fine-scale flood dynamics that are particularly important for flash flooding^{2,10,18}. In contrast, convection-permitting models that operate at kilometer-scale grid spacing^{17,19} start to resolve convective processes resulting in largely improved simulations of sub-daily extreme precipitation rates^{17,20–22}. Convection-permitting models, therefore, offer a valuable alternative for improved understanding of climate change impacts on flash flooding²³.

In this study, hourly data from a 13-year retrospective convection-permitting climate simulation with 4-km grid spacing and a 13-year future climate counterpart are used to investigate underlying future changes in flash floods. The retrospective simulation (also denoted as control run; CTL) downscales the ERA-Interim reanalysis²⁴ over the period from October 2000 to September 2013. The future simulation uses the Pseudo Global Warming approach (PGW)^{25,26} by adding climate change perturbations to the ERA-Interim boundary conditions and applies to the same period (2000–2013). Those perturbations are derived from an ensemble mean of 19 CMIP5 (Coupled Model Inter-comparison Project 5) GCMs under a high emission scenario (Representative Concentration Pathway: RCP8.5) during the period 2071–2100, compared to the reference period 1976–2005. The PGW simulation focuses on assessing more deterministic thermodynamic climate change impacts and does not allow studying the impacts of more uncertain changes in large-scale weather patterns²¹. It is noteworthy that the historical synoptic scale precipitation events are reproduced both in CTL and PGW owing to the use of spectral nudging²¹.

Several studies have verified the retrospective simulation (CTL) against precipitation climatology²¹, the simulation of hurricanes²⁷, atmospheric rivers²⁸, snowmelt²⁹, and extreme precipitation^{13,30,31}. In addition, we verified the CTL run with respect to the most commonly used precipitation dataset, National Centers for Environment Prediction Stage IV at four frequency-duration levels (i.e., 50-year 6-h, 50-year 24-h, 100-year 6-h, and 100-year 24-h events). For example, a 50-year term refers to frequency while 6-h refers to precipitation accumulation intervals. We aggregate our results to 17 “homogeneous” climate regions (the Bukovsky regions³²; Supplementary Fig. 1) to interpret regional climate differences on future flood changes.

Future flood risks pertaining to flash floods have not been thoroughly investigated under climate change scenarios, although the close relationship between rainfall rates and flood flashiness is well established by hydrometeorologists as a synoptic or mesoscale phenomenon³³. Flood resilience, termed as the ability to

mitigate the socioeconomic impacts of floods, has been brought up frequently in the wake of climate change³⁴. Taking advantage of the benefits of convection-permitting models, we quantify the impacts of climate change on future flood flashiness changes over the conterminous US (CONUS), which conveys information such as flood hazards, exposure, vulnerability, and impacts in the future⁵. In doing so, we use the CTL and PGW simulations to force a hydrologic model – the Ensemble Framework For Flash Flood Forecasting (EF5) which has been used operationally in the U.S. National Weather Service for flash flood forecasting across the CONUS and territories since 2017^{6,35–37}. For the analysis, the rainfall-flood event isolation and association are essentially needed to ensure the dependence between streamflow, precipitation, and antecedent soil moisture³⁸. Based on simulation outputs from 11 full calendar years (2001–2012) at an hourly time step, we extract flood events (defined by 2-year streamflow values determined by CTL) for both CTL and PGW runs. For each flood event, we identify the corresponding rainfall event using the Characteristic Points Method (CPM)³⁹.

This study hopes to provide quantitative assessments on changes in future flood-producing storms and flood flashiness, including geographical shifts in flash flood hotspots. It can be served as a basis for adapting nationwide flash flood planning strategies and calls on implementing climate-resilient mitigation measures for emerging flash flood hotspots.

Results

The results shown in the Supplementary Fig. 2 corroborate the satisfactory performance of CTL, as compared to Stage IV, with the correlation coefficient above 0.6. The simulated runoff by EF5 is compared with the community dataset – Global Streamflow Characteristic Dataset⁴⁰ at three percentiles (Quantiles 90, Quantiles 95, and Quantiles 99) (Supplementary Figs. 3 and 4), which verifies the efficacy of our model results. The rainfall-flood event association and calculation of the flashiness index (definition detailed in Methods section) and other characteristics are shown in Fig. 1a. The frequency change in Fig. 1b highlights that the US basins (e.g., the Southwest, Great Plains, and Prairie) – characterized by an intermittent streamflow regime, which is dominated by weak seasonality and local floods due to episodic precipitation events related to thunderstorms or fronts⁴¹ – will likely experience more floods in the PGW simulation. Small-to-medium size US rivers have a diverse response to warmer climates as their flood frequency changes range from –50 to 350 % (Fig. 1c). Large river basins, however, tend to be more stable with reduced uncertainty ranges. With that being said, small basins have more closely linked precipitation and streamflow, while floods in large basins are more likely to be modulated by antecedent basin wetness⁴².

Despite a general trend of increasing extreme precipitation at the end of this century in the PGW run^{30,31}, changes in the flood-producing event precipitation differ across climate divisions (Fig. 2). Significant positive percent changes (PC) in extreme precipitation are found across the Rockies (d and h) ($PC_{\text{mean}} = 34.5\%$; $PC_{99\%} = 28.5\%$) and Appalachia-Atlantic regions (p, n, and q) ($PC_{\text{mean}} = 24.7\%$; $PC_{99\%} = 21.9\%$). Flood events in these regions are typically related to spring snowmelt and rain-on-snow events^{4,28,43,44}. The flood-producing storms in the future, however, are likely associated with rainfall excess that is favored in a warming climate rather than snowfall³⁰. For these regions, future flood frequencies are nearly doubled (Fig. 1b).

Water vapor availability in the atmosphere in the central and eastern US plays an essential role in contributing to extreme precipitation changes^{11,14,44}. Additionally, extreme precipitation events are typically caused by specific storm types, e.g., (extra)tropical cyclones^{27,44}, mesoscale convective systems^{13,45}, and the North

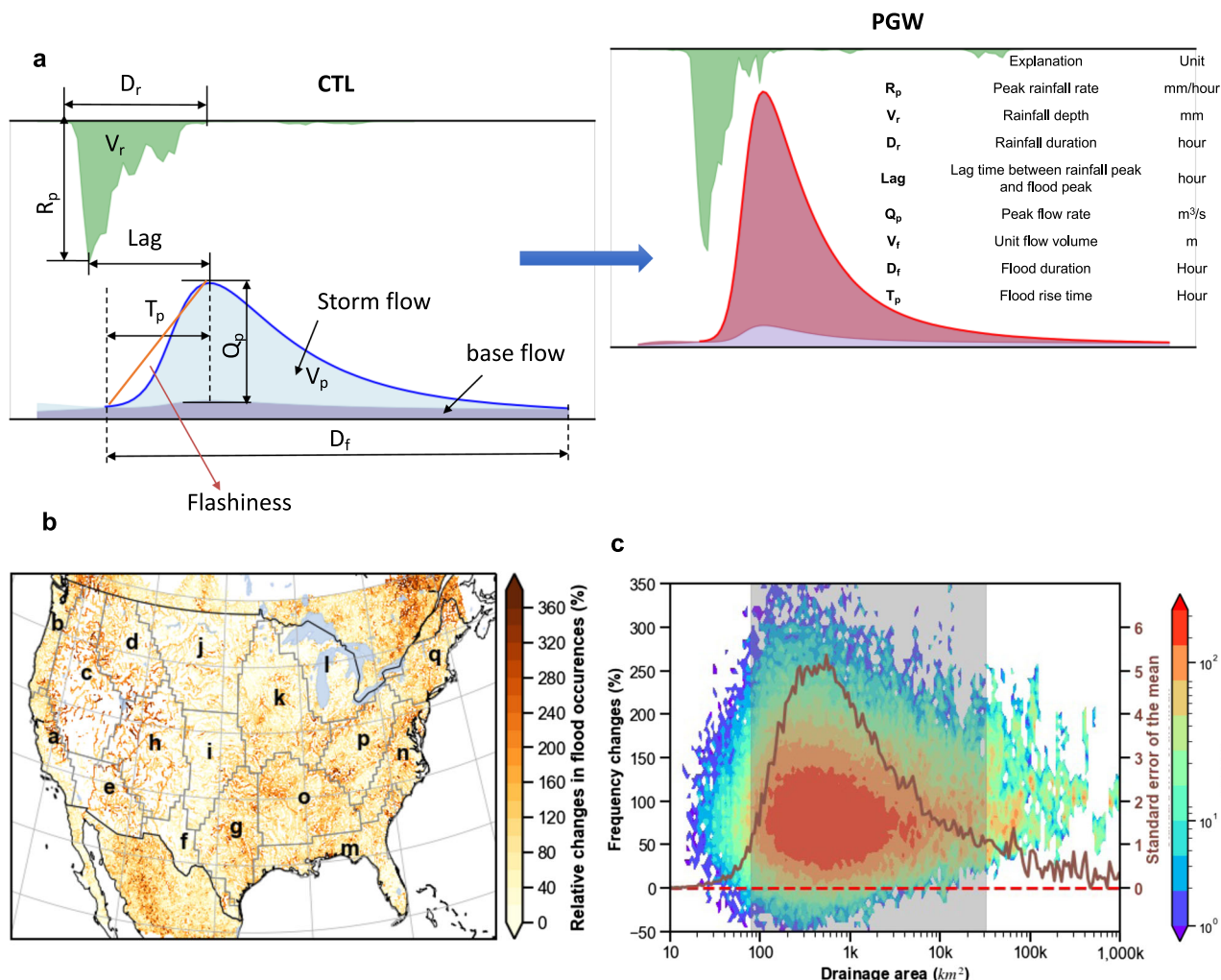


Fig. 1 Schematic view of rainfall-runoff event association at US HUC8 catchment scale. **a** illustration of calculated flood characteristics; **b** the percentage change of flood occurrences comparing the future (PGW) and retrospective analysis (CTL) at 1-km spatial resolution; **c** conditional plot of frequency changes against drainage area (shaded contour plot) and standard error of the mean in dark red line. Maps and figures are produced using the Python package Matplotlib and Cartopy.

American Monsoon (NAM)⁴⁴. The 26.6% increase of extreme precipitation in the eastern US agrees well within previous estimates of a 25–40% increase in mesoscale convective event rainfall³¹, which translates to 104% more frequent floods in the future (Fig. 2).

The largest change in flash-flood-producing precipitation occurs in the Southwest (e) ($PC_{mean} = +40.4\%$; $PC_{99\%} = 51.1\%$), where the main forcing agent for extreme precipitation is the NAM. The warm, moist air emanating from the Gulf of California fuels the storms and supports the “it never rains, but it pours” pattern in the arid climates, thereby leading to destructive flash floods^{3,7,11}. Although CMIP5 ensemble members project a weakening effect of NAM⁴⁶, its extreme precipitation rates are still likely to increase³¹. Correspondingly, future floods are becoming 123% more frequent there, representing the largest increase than other regions.

On the other hand, flood-producing extreme precipitation in the Pacific Southwest (a) and Northwest (b), Mezquital (f) regions is relatively insensitive to climate change, with only a few grid cells showing significant changes. Flood frequencies there increase by 67.1%, half of the probability of the aforementioned sensitive regions. Extreme precipitation is even projected to largely decrease in Mezquital (f) for both mean and extreme conditions (Fig. 2b, d), where the thermodynamic changes are likely limited by atmospheric moisture availability.

Consistent decreases of rainfall and flood event durations (D_r and D_f) are found across the CONUS climate divisions⁴⁷, measured by the fraction of events with negative changes (Fig. 3b, c), among which the Southern Plains (g; 55.8% and 56.7% of the total events), Deep South (o; 54.1% and 59.9% of the total events) and Southeast (m; 56.6% and 59.1% of the total events) have above-normal negative change events (52.1% and 52.4%) in the future. The shortened duration of rainfall and flooding could be partly explained by intense yet faster-moving storms in these regions¹³. In contrast, the majority of events with positive changes of peak rainfall rates and flow rates (R_p and Q_p) are located in the western US (Fig. 3b, c), i.e., Pacific Southwest (a; 79.6% and 75.9% of the total events), Pacific Northwest (b; 83.2% and 80.6% of the total events), Great Basins (c; 79.1% and 80.2% of the total events), and Northern Rockies (d; 80.8% and 80.2% of the total events). Similarly, these regions also see positive changes in rainfall and flood volumes (V_r and V_f , a – 67.2% and 68.1%; b – 72.6% and 72.3%; c – 70.8% and 72.8%; d – 69.9% and 71.6%). The future 7.5% decrease of lag time between rainfall and flood events is largely associated with antecedent soil moisture conditions and/or precipitation intensities, as the wetter soils and/or heavier precipitation rates accelerate flood-rise time^{5,36}. Specifically, humid regions with higher soil moisture content (e.g., Mid-Atlantic and Southeast) in the eastern US have a higher fraction of events

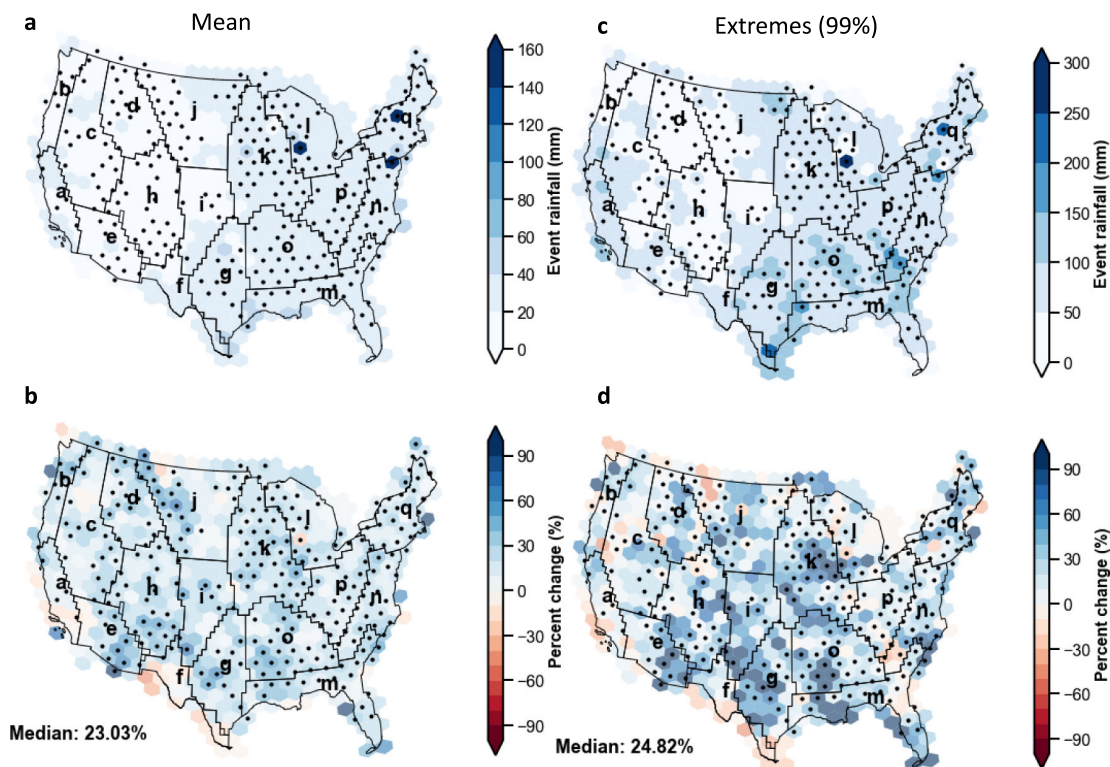


Fig. 2 Future increase in two-year flood-producing mean and 99th percentile event rainfall (mm) at 2.5-deg spatial resolution, grouped by Bukovsky climate divisions. **a** Retrospective mean event rainfall, **b** Percent changes (pseudo global warming minus retrospective simulation), **c** Retrospective extreme event rainfall (99th percentile), and **d** Percent changes (pseudo global warming minus retrospective simulation) in extreme event rainfall. The dots highlight significant changes with Kolmogorov-Smirnov two-side test for p -values < 0.05. Maps are produced using the Python package Matplotlib and Cartopy.

(65.1%) with reduced lag time than arid regions (e.g., Southwest and Mezquital; 60.3%), pointing to flashier hydrographs. Combined with factors such as peak flow rates (R_p) and time lag (lag), the flashiness index (flashiness) in the future is increased by 7.9% over the CONUS.

The present-day flashiness index distribution at the catchment scale (HUC8, Fig. 4a) is closely related to topography, climatology, river networks, and event characteristics (e.g., antecedent soil moisture, peak rainfall, and duration). The West Coast (1), Arizona (2), Rockies (3), Flash Flood Alley (4), and Appalachia (5) emerge as historical flash-flood hot spots (flashiness index > 0.8). We found similar clusters to the study of Sahari et al.⁷, in spite of a different approach. At the end of this century, the flashiness values are projected to increase across 87.4% of the HUC8 basins in the CONUS (Fig. 4b). Outside of the NAM-impacted region of Arizona, other flash-flood hot spots have a moderate increase of flashiness indices (4.1%). For these basins, the scaling rates, percent of flashiness index increase per warming temperature degree Celsius (averaged in each climate division), are close to zero (Fig. 4c). We suspect that the flashiness increase to a large extent is constrained by the physical limits of the basin geomorphology and land cover. For Arizona, however, the increase of flood-producing storms (Fig. 2) contributes to an increase in flashiness indices (+10.5%). In addition, the central US (e.g., Great Plains – j, i, g and Prairie – k), which used to be less prone to flash floods, has on average an 8.5% increase in flashiness indices, posing a potential threat to future floodwater management. In particular, the Prairie and Deep South will transition to hot spots in the future (Fig. 4b). We identify these regions (e.g., Southwest (+10.5%), Prairie (9.5%), Great Plains (+9.0%)) as climate sensitive regions to flash floods. Flood risk management including hard measures and soft measures is challenged by unawareness to potential flash flood

risks. Interestingly, positive flashiness changes are advancing northward (regions d, j, k, and l).

To link the changes in extreme precipitation and flashiness, Fig. 4d depicts the relationships among three variables – peak rainfall rates (R_p), rainfall depth (V_r), and rainfall duration (D_r). As expected, rainfall duration is weakly tied to the flashiness index because it is not the determining factor to either flood rising time or peak flow rates. Yet, both peak rainfall rates and rainfall volumes are positively correlated with flashiness. These two variables share a very similar rate of change (Fig. 4d) – around a 100% increase of extreme rainfall leads to a 10% increase of flashiness indices. When extreme rainfall change exceeds more than 120%, the flashiness index reaches a plateau. The plateau represents the physical limit of maximal channel conveyance which is jointly determined by catchments' geographical properties, including channel morphology, slope, land surface roughness, and soil properties^{43,48}.

This study conveys some similar conclusions found in other studies. For instance, decreasing trends in the duration of extreme rainfall and floods has been widely reported using either historical observations or climate simulations^{31,47}. High confidence can be obtained for increases in extreme precipitation amounts across the continental U.S., but there is variability due to model uncertainties and changes in regional weather systems. However, disagreements in streamflow responses to these precipitation changes are found across studies. For instance, a range of studies indicates decreasing trends in low-end flood frequencies based on historical observations, in which they deemphasize the dependence of floods on precipitation but rather emphasize the importance of antecedent catchment states^{49,50}. Even within climate model simulations, results can vary considerably over a given region, provided uncertainties in climate models, hydrologic model structures,

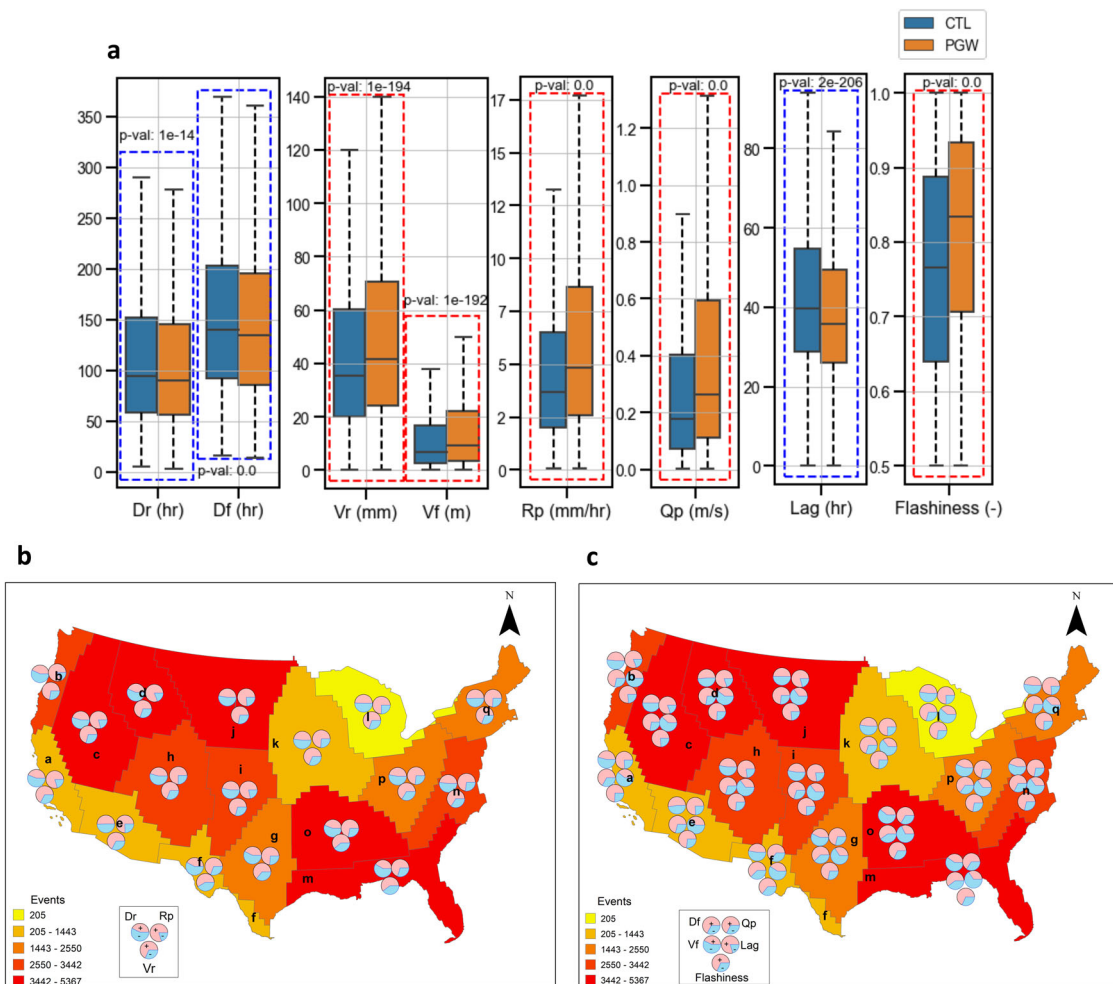


Fig. 3 Future rainfall/flood durations and rainfall-flood lag time are decreasing while rainfall/flood peak values, volumes, and flashiness index are increasing. **a** Boxplot of CONUS-wide statistics of rainfall-flood characteristics where blue dotted line indicates a future decrease while red dotted line indicates a future increase. Meaning of boxplot elements: central line: median, box limits: 25th and 75th percentiles, upper whisker: 75th percentile plus 1.5 times interquartile range, lower whisker: 25th percentile minus 1.5 times interquartile range. **b** Maps of the fraction of increase (red) or decrease (blue) for rainfall characteristics (Dr - duration, Rp - peak rates, and Vr - volume) at Bukovsky climate divisions. **c** Map of the fraction of increase (red) or decrease (blue) samples for flow characteristics (Df duration, Vf volume, Qp peak rates, Lag rainfall-flood-peak lag time, and Flashiness) at Bukovsky climate divisions. Shaded colors in **b** and **c** indicate the sample sizes. The blue (red) dashed box indicates a significant decrease (increase) of each feature (p -value < 0.05). The significance test is conducted by Kolmogorov-Smirnov test. Maps are produced using the ArcGIS.

and/or parameterizations^{2,11,20}. Our results differ from some other simulations regarding flood magnitudes because firstly we use the high-end emissions scenario – RCP8.5 – that dramatically warms and invigorates the atmosphere. Second, unlike both dynamic and thermodynamic evolution of weather patterns in GCMs, our PGW scheme only permits investigation of the less uncertain component of thermodynamic changes to the atmosphere. Third, the hourly and 4-km resolution model simulations resolve convective-scale weather phenomena that are only parameterized in GCMs. Precipitation simulations are more realistic, conditioned on the thermodynamic changes associated with RCP 8.5, and thus can be applied in a hydrologic modeling context. To be noted, we only investigated the rainfall indices based on rates, volume, time-to-peak, and duration. Other proper indices such as ratios of peak rainfall rates and volumes could be meaningful to interpret the dynamic evolution of rainfall storms.

This work by no means intends to deliver an exhaustive depiction of future floods. The PGW approach is based on a high-end emissions scenario (RCP8.5), which may or may not be realized in the future. Furthermore, anthropogenic impacts such as Land Use Land Cover type changes and river regulations are

not considered in the modeling settings. One of the reasons is the uncertain prediction of such processes, even though some standards are being developed as a community effort⁵¹. The Land Use Land Cover changes especially for urban areas could even worsen the future situation by reshaping and magnifying hydrologic responses – less infiltration and more surface runoff⁵². It is also reported that urbanization exacerbates extreme rainfall due to increased aerosols and altered circulations from urban heat island. Therefore, our results could serve as a basis or benchmark if not the worst-case scenario.

In summary, there is a pressing need to understand how future flood flashiness responds to climate change for early mitigation and adaptation measures. Here we present results that translate rainfall-flood event changes from convection-permitting climate simulations to changes in flood flashiness. Four main findings presented in this study include:

1. A CONUS-wide 7.9% increase in future flood flashiness means that future floods will onset more rapidly with higher peak runoff resulting in even shorter opportunities for early warning.

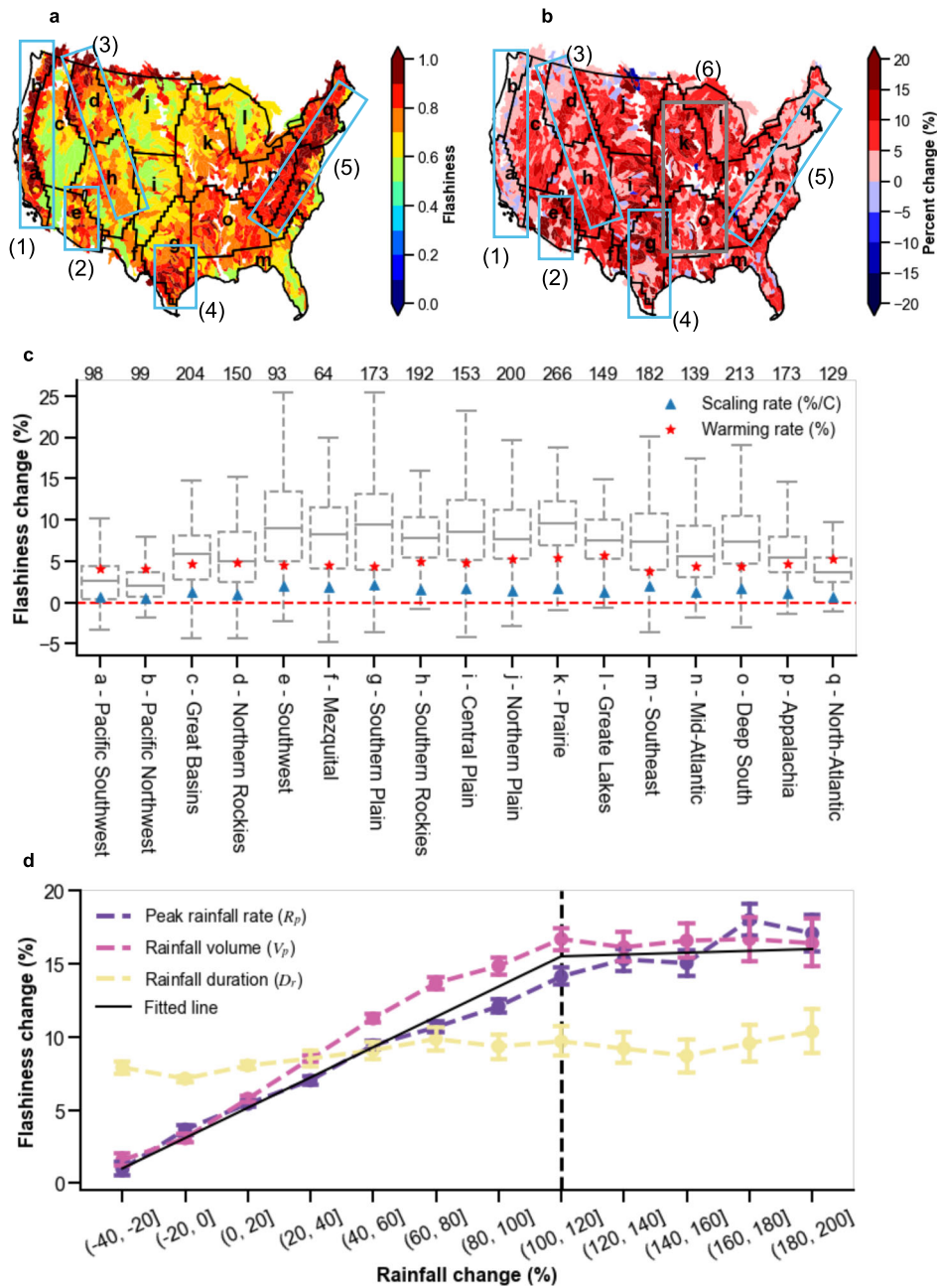


Fig. 4 Future flashiness indices will increase by 7.9%, while Southwest being affected the most (10.5%). **a** Present-day flashiness indices driven by the retrospective analysis (blue box encompass historical flash flood hot spots identified from Sahari et al⁷). **b** Future flashiness changes of the difference of PGW run and CTL run (blue box encompasses historical flash flood hot spots, and gray box shows the emerged future flood hot spot). **c** Changes of flashiness indices for all climate divisions, accompanied by warming rate and scaling rate. Meaning of boxplot elements: central line: median, box limits: 25th and 75th percentiles, upper whisker: 75th percentile plus 1.5 times interquartile range, lower whisker: 25th percentile minus 1.5 times interquartile range. **d** Plot regarding binned rainfall changes (including rates - purple line, volumes - red line, and duration - yellow line) on the x axis versus flashiness indices changes on the y axis. Upper and lower whiskers indicate the 75th and 25th percentile, respectively. Maps and figures are produced using the Python package Matplotlib and Cartopy.

- Regions outside of the North American Monsoon have moderate increases in flashiness (+4.1%) in a warmer climate. However, floods in the Southwest become much flashier (+10.5%).
- The central US have an on average an 8.5% increase in flood flashiness. Particularly, basins in the Deep South and Prairie will transition into new flash flood hot spots in a warmer, future climate.

- Future flash flood risks are advancing northwards (Northern Rockies, Northern Plains, and Prairie), which poses challenges to local flood resilience measures.

This study shows a pressing need to adapt to climate change and mitigate future flood risks because of an overall increase of flashiness over the CONUS, resulting in less response time for local communities to react. Reassessment of current floodwater management and planning for future flood risk is necessary for

judging current standards⁵³. More critically, emerging flash flood hot spot regions will be facing unprecedented challenges because of the historically unpreparedness of flood impacts in conjunction with aging infrastructure and outdated flood risk measures⁵⁴. Potential future studies can examine the seasonal cycles and spatial extent of both storms and floods to reveal the spatio-temporal correlation between the two. In addition, it is critical to consider more anthropogenic influences on floods such as river controls and increased urbanization^{55,56}.

Methods

Datasets. To evaluate the performance of retrospective simulations, we curated historical extreme rainfall events archived by the Colorado State University Real-Time Weather Data (http://schumacher.atmos.colostate.edu/precip_monitor/50y24h/event_images/year_list.php). The extreme precipitation thresholds are determined by NOAA Atlas 14, which is a gridded product that is derived by over a hundred-year rainfall gauge dataset and fitted with an assumed distribution. The hourly precipitation data is based on the National Centers for Environmental Prediction Stage IV radar-gauge merged product from the University Cooperation for Atmospheric Research/National Center for Atmospheric Research Earth Observing Laboratory. Because Stage IV hourly data availability on the West Coast is generally under 60%, the evaluation extent is confined to the Midwest and the eastern U.S. There is a systematic bias (>10%; underestimation) for precipitation between Stage IV and CTL, partly due to imperfect physical schemes, boundary feedbacks for regional climate model (RCM) simulations, and climate variability⁵⁷.

The Global Streamflow Characteristics Dataset, which provides extreme streamflow values at daily resolution, is used to verify our hydrologic simulations⁴⁰. This dataset is a machine-learning-aided product, training catchment streamflow characteristics based on a set of climate and physiographic features with historical data from 9169 USGS stream gauges⁵⁸. The produced results have been assessed against five global hydrologic models for further independent evaluation. A negative systematic bias (>8%) for surface runoff persists as propagated from the aforementioned precipitation bias, but other contributing factors within the hydrologic model simulations (i.e., calibrated parameters based on different forcing datasets, uncertainties in hydrologic model structure) slightly compensate for the precipitation bias.

Climate simulations. Two 4-km and hourly datasets from climate simulations are analyzed and used as forcing for hydrologic models. Such simulations are created with the community Weather Research and Forecast (WRF) model Version 3.4.1 (see Liu et al.²¹ for reference), encompassing the whole CONUS and portions of Canada and Mexico. The retrospective simulation (CTL) from 1 October 2000 to 30 September 2013 downscales ERA-Interim reanalysis data²⁴, with spectral nudging being applied. The future climate simulation uses the Pseudo Global Warming approach (PGW)^{25,26} by perturbing the climatic boundary conditions (horizontal wind, geopotential heights, temperature, specific humidity, sea surface temperature, soil temperature, sea level pressure, and sea ice). An ensemble mean of climate signals from 19 CMIP5 models for the period 2070 to 2100, relative to the reference period 1976 to 2005, is added to ERA-Interim boundary conditions under RCP8.5. In principle, the essence of the PGW run is to assess thermodynamic climate change signals in contrast to changes in large-scale weather patterns such as shifts of the large-scale storm tracks and North Atlantic jet stream⁵⁹. The benefits of PGW simulations are that systematic GCM errors are mostly excluded in the downscaled simulation, and the effects from climate internal variability on climate change signals can be thus ignored. Previous model comparisons between PGW run and CMIP5 reveal similar climate change patterns over the CONUS²¹.

Hydrologic models. In this study, the simulated retrospective and future precipitation events are taken separately as forcing to drive a hydrologic model. We use the widely recognized flash flood forecast model – the Ensemble Framework For Flash Flood Forecasting (EF5), developed jointly at the University of Oklahoma and NOAA National Severe Storms Laboratory (Flamig et al.³⁵). The EF5 model has been in operation for real-time flash flood forecast across the CONUS and territories at 1-km spatial resolution and updates every 10 min⁶. Forecasters in the U.S. National Weather Services (NWS) utilize this product to issue flash flood warnings. The model is developed across operating systems (Linux, macOS, and Windows) and is publicly available at <https://github.com/HyDROSLab/EF5>.

In this study, we choose the subset hydrologic model – Coupled Routing and Excess STorage (CREST) V2.1³⁵ and routing model – kinematic wave within the EF5 framework to simulate streamflow at 1 km spatial resolution and hourly temporal resolution from 2001 to 2011. The nearest neighbor method is used to downscale precipitation data at 4 km to be consistent with topographic resolution at 1 km. The distributed parameters for the CREST and the kinematic wave model remain the same as the operational runs. To separate errors from hydrologic models and forcing input, we similarly run EF5 using Stage IV as precipitation inputs for the same period (2001–2011). From the previous model evaluation, this

model is generally suited for flash floods or heavy-rainfall-induced floods while not modeling snowmelt events or rain-on-snow events³⁵.

Hydrograph separation and rainfall-flood event association. Prior to comparisons, the time series of outputs from hydrologic models (i.e., streamflow and basin-average rainfall rates) are extracted at each HUC8 basin over the CONUS. Then, flood events are identified according to the following two criteria. First, peak streamflow should exceed the threshold for a 2-year flood, typically considered as a bankfull condition¹⁸. The two-year flood is determined by fitting annual maximum streamflow into a log-Pearson Type III distribution, which is a conventional method used by the U.S. Geological Survey, and extracting values at 2-year exceedance. Second, to specifically focus on flashier floods, we set a threshold for the flood rising slope, peak streamflow divided by rising time. This threshold is computed as a function of upstream flow accumulation values and is empirically suggested in Chow et al.⁶⁰, meaning that large basins allow more time to be considered as flash floods than small basins. For rainfall-flood event association, we use the Characteristic Point Method, which has been applied to compile a comprehensive flood database over the CONUS³⁹. The Characteristic Point Method firstly separates storm event flow and base flow with the filtered revised constant k method, which is a hybrid method of the revised constant k and recursive digital filter. Secondly, event identification is achieved through linking separated flow events and rainfall events within a search window. For a detailed description and application of the method, the reader is referred to Mei and Anagnostou⁶¹. Some event signatures are exported to describe the matched rainfall and flood events, such as rainfall duration (D_r), peak rainfall rate (R_p), rainfall volume (V_r), flood duration (D_f), peak flow rate (Q_f), flood volume (V_f), rainfall-flood lag time (Lag). On top of these signatures, we calculate the flood flashiness index per event with respect to flood rising time and peak flow rate as shown in Eq. 1⁷.

$$\text{Flashiness}_{s,i,j} = \frac{Q_{p,s,i,j} - Q_{b,s,i,j}}{A_i T_{b,s,i,j}} \quad (1)$$

where the subscripts s, i, j indicate each scenario (CTL or PGW), HUC8 basin, and flood event; Q_p and Q_b refer to the peak flow and base flow, and A and T are the drainage area and flood rising time. The baseflow is calculated following the Characteristic Point Method, which uses filtered revised constant k method – a combination of revised constant k and recursive digital filter – to separate storm flow and baseflow. To scale the flashiness index values between 0 and 1, we fit a collection of flashiness values with an empirical cumulative distribution function (ecdf). Then the basin-level flashiness index is calculated as the median value of all event-based flashiness values within each basin. Results of flashiness index calculated using our model outputs are compared to the study of Saharia et al.⁷ at U.S. Geological Survey stream gauge locations (Supplementary Fig. 5).

Data availability

The climate simulation data⁶² is downloaded from the NCAR (National Center for Atmospheric Research) Research Data Archive (<https://rda.ucar.edu/datasets/ds612.0>). Underlying data⁶³ for the main manuscript figures can be accessed at <https://doi.org/10.6084/m9.figshare.19127186.v1>.

Code availability

The EF5/CREST model^{35,64} is publicly available from Zenodo (<https://doi.org/10.5281/zenodo.4009759>) and Github (<https://github.com/HyDROSLab/EF5>). The Matlab code for Characteristic Point Method can be accessed from <https://ucwater.engr.uconn.edu/models-data/#>.

Received: 14 October 2021; Accepted: 21 February 2022;

Published online: 06 April 2022

References

- Gourley, J. J. et al. A Unified Flash Flood Database across the United States. *Bull. Am. Meteorol. Soc.* **94**, 799–805 (2013).
- Hirabayashi, Y. et al. Global flood risk under climate change. *Nat. Clim. Change* **3**, 816–821 (2013).
- Khajehei, S. et al. A place-based assessment of flash flood hazard and vulnerability in the contiguous United States. *Sci. Rep.* **10**, 448 (2020).
- Li, Z. et al. A multi-source 120-year U.S. flood database with a unified common format and public access. *Earth Syst. Sci. Data* **13**, 3755–3766 (2021).
- Merz, B. et al. Causes, impacts and patterns of disastrous river floods. *Nat. Rev. Earth Environ.* **2**, 592–609 (2021).
- Gourley, J. J. et al. The FLASH Project: improving the tools for flash flood monitoring and prediction across the United States. *Bull. Am. Meteorol. Soc.* **98**, 361–372 (2017).
- Saharia, M. et al. Mapping flash flood severity in the United States. *J. Hydrometeorol.* **18**, 397–411 (2017).

8. Ahmadi, A. & Moradkhani, H. A data-driven analysis of flash flood hazard, fatalities, and damages over the CONUS during 1996–2017. *J. Hydrol.* **578**, 124106 (2019).
9. Fowler, H. J., Wasko, C. & Prein, A. F. Intensification of short-duration rainfall extremes and implications for flood risk: current state of the art and future directions. *Phil. Trans. R. Soc. A Math. Phys. Eng. Sci.* **379**, 20190541 (2021).
10. Swain, D. L. et al. Increased flood exposure due to climate change and population growth in the United States. *Earth's Future* **8**, e2020EF001778 (2020).
11. Tabari, H. Climate change impact on flood and extreme precipitation increases with water availability. *Sci. Rep.* **10**, 13768 (2020).
12. Allen, M. R. & Ingram, W. J. Constraints on future changes in climate and the hydrologic cycle. *Nature* **419**, 224–232 (2002).
13. Prein, A. F. et al. Increased rainfall volume from future convective storms in the US. *Nat. Clim. Change* **7**, 880–884 (2017).
14. Westra, S. et al. Future changes to the intensity and frequency of short-duration extreme rainfall. *Rev. Geophys.* **52**, 522–555 (2014).
15. Fowler, H. J. et al. Anthropogenic intensification of short-duration rainfall extremes. *Nat. Rev. Earth Environ.* **2**, 107–122 (2021).
16. Zhang, B., Wang, S. & Wang, Y. Probabilistic projections of multidimensional flood risks at a convection-permitting scale. *Water Resour. Res.* **56**, e2020WR028582 (2020).
17. Prein, A. F. et al. A review on regional convection-permitting climate modeling: demonstrations, prospects, and challenges. *Rev. Geophys.* **53**, 323–361 (2015).
18. Bates, P. D. et al. Combined modelling of US fluvial, pluvial and coastal flood hazard under current and future climates. *Water Resour. Res.* **56**, e2020WR028673 (2020).
19. Clark, P., Roberts, N., Lean, H., Ballard, S. P. & Charlton-Perez, C. Convection-permitting models: a step-change in rainfall forecasting. *Meteorol. Appl.* **23**, 165–181 (2016).
20. Clark, M. P. et al. Characterizing uncertainty of the hydrologic impacts of climate change. *Curr. Clim. Change Rep.* **2**, 55–64 (2016).
21. Liu, C. et al. Continental-scale convection-permitting modeling of the current and future climate of North America. *Clim. Dyn.* **49**, 71–95 (2017).
22. Wehner, M. F., Arnold, J. R., Knutson, T., Kunkel, K. E. & LeGrande, A. N. *Climate Science Special Report: Fourth National Climate Assessment*. Vol. I. Ch. 8 (U.S. Global Change Research Program, Washington, 2017).
23. Younis, J., Anquetin, S. & Thielen, J. The benefit of high-resolution operational weather forecasts for flash flood warning. *Hydrol. Earth Syst. Sci.* **12**, 1039–1051 (2008).
24. Dee, D. P. et al. The ERA-Interim reanalysis: configuration and performance of the data assimilation system. *Q. J. R. Meteorol. Soc.* **137**, 553–597 (2011).
25. Schär, C., Frei, C., Lüthi, D. & Davies, H. C. Surrogate climate-change scenarios for regional climate models. *Geophys. Res. Lett.* **23**, 669–672 (1996).
26. Rasmussen, R. et al. Climate change impacts on the water balance of the Colorado headwaters: High-resolution regional climate model simulations. *J. Hydrometeorol.* **15**, 1091–1116 (2014).
27. Gutmann, E. D. et al. Changes in hurricanes from a 13-Yr convection-permitting pseudo-global warming simulation. *J. Clim.* **31**, 3643–3657 (2018).
28. Dougherty, E., Sherman, E. & Rasmussen, K. L. Future changes in the hydrologic cycle associated with flood-producing storms in California. *J. Hydrometeorol.* **21**, 2607–2621 (2020).
29. Musselman, K. N. et al. Projected increases and shifts in rain-on-snow flood risk over western North America. *Nat. Clim. Change* **8**, 808–812 (2018).
30. Dougherty, E. & Rasmussen, K. L. Changes in future flash flood-producing storms in the United States. *J. Hydrometeorol.* **21**, 2221–2236 (2020).
31. Prein, A. et al. The future intensification of hourly precipitation extremes. *Nat. Clim. Change* **7**, 48–52 (2017).
32. Bukovsky, M. S. 2011: *Masks for the Bukovsky regionalization of North America*, Regional Integrated Sciences Collective, Institute for Mathematics Applied to Geosciences, National Center for Atmospheric Research, Boulder, CO. Downloaded 2021-07-05. <http://www.narccap.ucar.edu/contrib/bukovsky/>.
33. Maddox, R. A., Chappell, C. F. & Hoxit, L. R. Synoptic and meso-scale aspects of flash flood events. *Bull. Am. Meteorol. Soc.* **60**, 115–123 (1979).
34. McClymont, K., Morrison, D., Beevers, L. & Carmen, E. Flood resilience: a systematic review. *J. Environ. Plan. Manag.* **63**, 1151–1176 (2020).
35. Flamig, Z. L., Vergara, H. & Gourley, J. J. The ensemble framework for flash flood forecasting (EF5) v1.2: description and case study. *Geosci. Model Dev.* **13**, 4943–4958 (2020).
36. Li, Z. et al. CREST-iMAP v1.0: A fully coupled hydrologic-hydraulic modeling framework dedicated to flood inundation mapping and prediction. *Environ. Model. Softw.* **141**, 105051 (2021).
37. Xue, X. et al. Statistical and hydrological evaluation of TRMM-based Multi-satellite Precipitation Analysis over the Wangchu Basin of Bhutan: are the latest satellite precipitation products 3B42V7 ready for use in ungauged basins? *J. Hydrol.* **499**, 91–99 (2013).
38. Wasko, C., Sharma, A. & Lettenmaier, D. P. Increases in temperature do not translate to increased flooding. *Nat. Commun.* **10**, 5676 (2019).
39. Shen, X., Mei, Y. & Anagnostou, E. N. A comprehensive database of flood events in the contiguous United States from 2002 to 2013. *Bull. Am. Meteorol. Soc.* **98**, 1493–1502 (2017).
40. Beck, H. A global map of mean annual runoff based on discharge observations from large catchments. *Zenodo*. <https://doi.org/10.5281/zenodo.44782> (2016).
41. Brunner, M. I., Melsen, L. A., Newman, A. J., Wood, A. W. & Clark, M. P. Future streamflow regime changes in the United States: assessment using functional classification. *Hydrol. Earth Syst. Sci.* **24**, 3951–3966 (2020).
42. Ivancic, T. J. & Shaw, S. B. Examining why trends in very heavy precipitation should not be mistaken for trends in very high river discharge. *Clim. Change*. **133**, 681–693 (2015).
43. Villarini, G. On the seasonality of flooding across the continental United States. *Adv. Water Resour.* **87**, 80–91 (2016).
44. Kunkel, K. E. et al. Monitoring and understanding trends in extreme storms: state of knowledge. *Bull. Am. Meteorol. Soc.* **94**, 499–514 (2013).
45. Diffenbaugh, N. S., Scherer, M. & Trapp, R. J. Robust increases in severe thunderstorm environments in response to greenhouse forcing. *Proc. Natl. Acad. Sci. USA* **110**, 16361–16366 (2013).
46. Cook, B. I. & Seager, R. The response of the North American Monsoon to increased greenhouse gas forcing. *J. Geophys. Res. Atmos.* **118**, 1690–1699 (2013).
47. Wasko, C., Nathan, R., Stein, L. & O'Shea, D. Evidence of shorter more extreme rainfalls and increased flood variability under climate change. *J. Hydrol.* **603**, 126994 (2021).
48. Berghuijs, W. R., Woods, R. A., Hutton, C. J. & Sivapalan, M. Dominant flood generating mechanisms across the United States. *Geophys. Res. Lett.* **43**, 4382–4390 (2016).
49. Sharma, A., Wasko, C. & Lettenmaier, D. P. If precipitation extremes are increasing, why aren't floods? *Water Resour. Res.* **54**, 8545–8551 (2018).
50. Wasko, C., Sharma, A. & Lettenmaier, D. P. Increases in temperature do not translate to increased flooding. *Nature comm.* **10**, 1–3 (2019).
51. Riahi, K. et al. The Shared Socioeconomic Pathways and their energy, land use, and greenhouse gas emissions implications: an overview. *Glob. Environ. Change*. **42**, 153–168 (2017).
52. Zhang, W. et al. Urbanization exacerbated the rainfall and flooding caused by hurricane Harvey in Houston. *Nature* **563**, 384–388 (2018).
53. Lopez-Cantu, T. & Samaras, C. Temporal and spatial evaluation of stormwater engineering standards reveals risks and priorities across the United States. *Environ. Res. Lett.* **13**, 074006 (2018).
54. Wright, D. B., Bosma, C. D. & Lopez-Cantu, T. U.S. hydrologic design standards insufficient due to large increases in frequency of rainfall extremes. *Geophys. Res. Lett.* **46**, 8144–8153 (2019).
55. Blum, A. G., Ferraro, P. J., Archfield, S. A. & Ryberg, K. R. Causal effect of impervious cover on annual flood magnitude for the United States. *Geophys. Res. Lett.* **47**, e2019GL086480 (2020).
56. Wyzga, B. Methods for studying the response of flood flows to channel change. *J. Hydrol.* **198**, 271–288 (1997).
57. Ehret, U., Zehe, E., Wulfmeyer, V., Warrach-Sagi, K. & Liebert, J. HESS Opinions “Should we apply bias correction to global and regional climate model data?”. *Hydrol. Earth Syst. Sci.* **16**, 3391–3404 (2012).
58. Beck, H. E., de Roo, A. & van Dijk, A. I. J. M. Global maps of streamflow characteristics based on observations from several thousand catchments. *J. Hydrometeorol.* **16**, 1478–1501 (2015).
59. Barnes, E. A. & Polvani, L. Response of the midlatitude jets, and of their variability, to increased greenhouse gases in the CMIP5 models. *J. Clim.* **26**, 7117–7135 (2013).
60. Chow, V. T., Maidment, D. R. & Mays, L. W. *Applied Hydrology* (McGraw-Hill, 1988).
61. Mei, Y. & Anagnostou, E. N. A hydrograph separation method based on information from rainfall and runoff records. *J. Hydrol.* **523**, 636–649 (2015).
62. Rasmussen, R. & Liu, C. High resolution WRF simulations of the current and future climate of North America. *Research Data Archive at the National Center for Atmospheric Research, Computational and Information Systems Laboratory*. <https://doi.org/10.5065/D6V40SXP>. Accessed 09/01/2020 (2017).
63. Li, Z. Flashier Floods over the Conterminous US under a Changing Climate. *figshare Dataset*. <https://doi.org/10.6084/m9.figshare.19127186.v1> (2022).
64. Flamig, Z. HyDROSLab/EF5-US-Parameters: EF5 parameters for USA (v1.0.0). *Zenodo*. <https://doi.org/10.5281/zenodo.4009759> (2020).

Acknowledgements

The first author is sponsored by the University of Oklahoma Hydrology and Water Security (HWS) program (<https://www.ouhydrologyonline.com/>) and Graduate College Hoving Fellowship.

Author contributions

Z.L., J.J.G., and Y.H. conceived this study; Z.L., M.C., S.G., C.L., and A.F.P. designed the methodology and implemented the experiments; C.L. contributed datasets. Z.L. wrote the codes for analysis and original draft; all the co-authors reviewed and edited this manuscript.

Competing interests

The authors declare no competing interests.

Additional information

Supplementary information The online version contains supplementary material available at <https://doi.org/10.1038/s43247-022-00409-6>.

Correspondence and requests for materials should be addressed to Yang Hong.

Peer review information *Communications Earth & Environment* thanks the anonymous reviewers for their contribution to the peer review of this work. Primary Handling Editors: Rahim Barzegar, Heike Langenberg. Peer reviewer reports are available.

Reprints and permission information is available at <http://www.nature.com/reprints>

Publisher's note Springer Nature remains neutral with regard to jurisdictional claims in published maps and institutional affiliations.



Open Access This article is licensed under a Creative Commons Attribution 4.0 International License, which permits use, sharing, adaptation, distribution and reproduction in any medium or format, as long as you give appropriate credit to the original author(s) and the source, provide a link to the Creative Commons license, and indicate if changes were made. The images or other third party material in this article are included in the article's Creative Commons license, unless indicated otherwise in a credit line to the material. If material is not included in the article's Creative Commons license and your intended use is not permitted by statutory regulation or exceeds the permitted use, you will need to obtain permission directly from the copyright holder. To view a copy of this license, visit <http://creativecommons.org/licenses/by/4.0/>.

© The Author(s) 2022